Electronic supplementary information

A Positional Isomerism Strategy of Fluorophenyl Substituents in Self-Assembled Monolayers for Perovskite Solar Cells

Xing Liu, Hang Deng, Xiaorui Liu*

Key Laboratory of Luminescence Analysis and Molecular Sensing Ministry of Education, School of Chemistry and Chemical Engineering, Southwest University, Chongqing 400715, P. R. China.

*Corresponding author(s): Email: liuxiaorui@ swu.edu.cn

S1. Computational Details

The ground-state geometries of the target molecules, ZY4-ZY6 and 4PACz, were optimized at the B3LYP/6-31G(d,p) level. The optimized geometries were validated by the absence of imaginary frequencies, confirming them as local energy minima. Subsequently, the energies of the frontier molecular orbitals (FMOs) were determined. The optical properties of ZY4-ZY6 and 4PACz were calculated using time-dependent density functional theory (TD-DFT) at the B3LYP/6-31G(d,p) level, with the ethanol solvent environment simulated using the polarizable continuum model (PCM). Organic molecular reorganization energy includes both internal and external parts. The internal part is defined by the energy of nuclear rearrangement from initial to final coordinates. Since the external reorganization energy is typically small and can be ignored for most organic molecules, we focus herein on calculating the internal hole reorganization energy. The hole reorganization energy (λ_h) was determined using the adiabatic potential energy surface method at the B3LYP/6-31G(d,p) level. All DFT and TD-DFT

calculations were carried out employing the Gaussian 09 software package.[1]

Classical molecular dynamics (MD) simulations of the Perovskite/SAMs/NiO_x interface were performed using the GROMACS software package.[2] The simulations were conducted under the NVT ensemble, with the equations of motion integrated using the Velocity Verlet algorithm and a time step of 1 fs. Long-range electrostatic and van der Waals interactions were handled with the PME method and a dispersion correction, respectively, using a 1.2 nm cutoff. The perovskite and NiO_x were described by the UFF force field, whereas the SAMs were modeled with the GAFF force field,[3,4] with their atomic charges assigned via RESP fitting to DFT-derived electrostatic potentials. The simulation model was constructed as follows: the perovskite surface was composed of an 8×8×2 supercell of $FAPbI_3$, while the NiO_x surface was formed from a 12×12×2 supercell of NiO_x. A SAMs layer with a thickness of 20 Å was incorporated between them. Four distinct heterostructure models were constructed, each incorporating 30 molecules of ZY4, ZY5, ZY6, or 4PACz, respectively. These SAM molecules were randomly placed on the NiO_x surface using the Packmol tool to ensure unbiased sampling. The system was initially equilibrated at 298 K for 0.1 ns, followed by a temperature increase to 300 K for subsequent production simulations. A central molecule was selected from the monolayer, and two adjacent molecules exhibiting significant π–π stacking interactions with the central unit were identified to define the hole-transport pathway. The charge transfer integral (v), charge transfer rate (k), and hole mobility (u_h) were computed using the ADF software package. Electronic coupling matrix elements were evaluated at the PW91/TZP level of theory.[5,6] Geometry optimization of the SAM/NiO_x interface was performed within the VASP framework,[7-9] employing the GGA-PBE functional. The underlying substrate was comprised of a 3×3×2 supercell of $FAPbI_3$ (001) and a 3×2×2 supercell of NiO_x (100). To enhance

computational efficiency, the bottom layers of the NiO_x substrate were removed, and spin polarization was explicitly included for Ni atoms. Furthermore, the electron wavefunctions were expanded using a plane-wave basis set with a kinetic energy cutoff of 400 eV. The Brillouin zone was sampled using only the Gamma-point (1×1×1). To prevent unphysical interactions between periodic replicas, a vacuum layer of 20 Å was introduced in the direction normal to the Perovskite/ NiO_x surface. The convergence criterion for the electronic self-consistent field (SCF) iteration was set to 1.0×10^{-4} eV/atom. A subsequent non-self-consistent calculation was then performed, and the resulting charge density file was processed to generate the charge density difference (CDD) map. The adsorption energy is calculated by the formula: $E_{ads}=E_{total}-E_{slab}-E_{molecule}$ where E_{total}, E_{slab}, and $E_{molecule}$ represent the total energy of the adsorption system, the energy of the bare slab, and the energy of the isolated molecule, respectively.

The wavefunctions of the dimers involving ZY4 and ZY5 were first computed at the B3LYP-D3(BJ)/6-31G(d,p) level. Subsequently, the intermolecular interactions were visualized using the Independent Gradient Model based on Hirshfeld partition (IGMH) as implemented in the Multiwfn program.[10]

S2. Figures

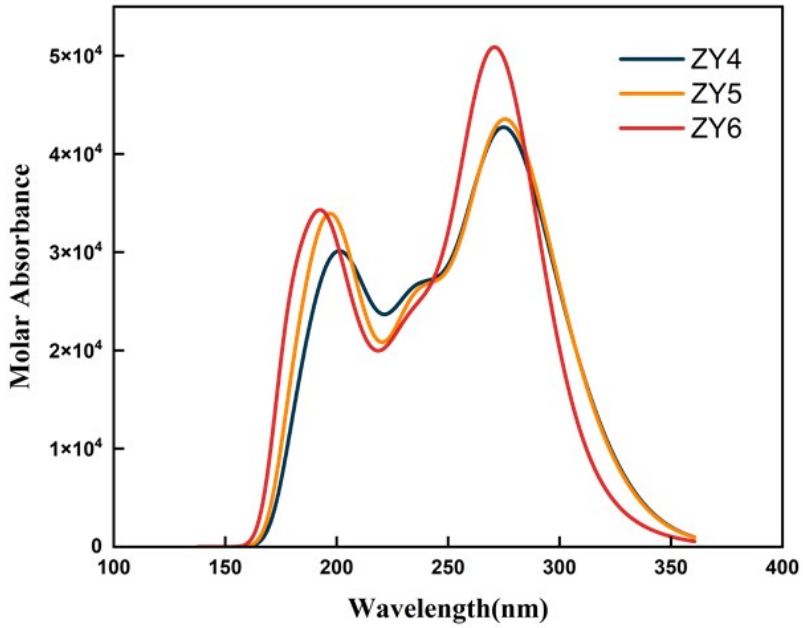

Fig.S1 Simulated absorption spectra of molecules ZY4-ZY6 using the TD-B3LYP /6-31G(d,p) functional and basis set in Ethanol.

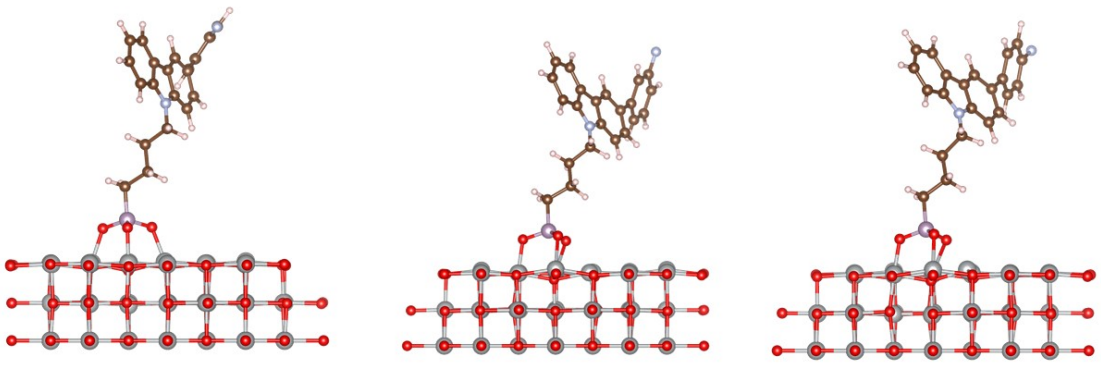

Fig.S2 The structures of ZY4, ZY5, and ZY6 on the NiO_x surface were optimized.

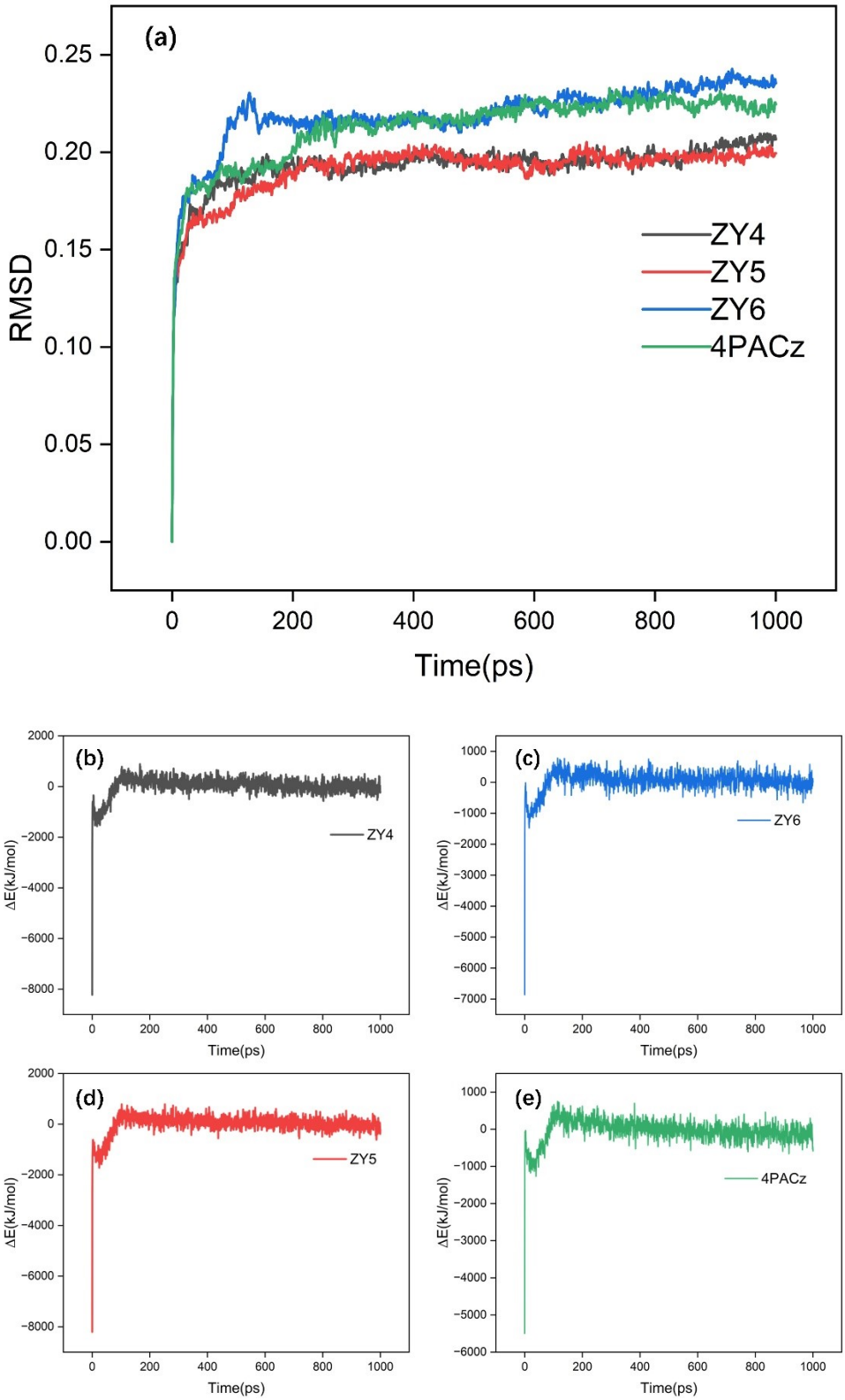

Fig.S3 (a) Root Mean Square Deviation plot of ZY4-ZY6 and 4PACz. (b)~(e) Average energy change ΔE plots of ZY4-ZY6 and 4PACz.

References

1 M. J. Frisch, G. W. Trucks, H. B. Schlegel, G. E. Scuseria, M. A. Robb, J. R. Cheeseman, G. Scalmani, V. Barone, B. Mennucci, G. A. Petersson, H. Nakatsuji, M. Caricato, X. Li, H. P. Hratchian, A. F. Izmaylov, J. Bloino, G. Zheng, J. L. Sonnenberg, M. Hada, M. Ehara, K. Toyota, R. Fukuda, J. Hasegawa, M. Ishida, T. Nakajima, Y. Honda, O. Kitao, H. Nakai, T. Vreven, J. A. Montgomery, Jr., J. E. Peralta, F. Ogliaro, M. Bearpark, J. J. Heyd, E. Brothers, K. N. Kudin, V. N. Staroverov, R. Kobayashi, J. Normand, K. Raghavachari, A. Rendell, J. C. Burant, S. S. Iyengar, J. Tomasi, M. Cossi, N. Rega, J. M. Millam, M. Klene, J. E. Knox, J. B. Cross, V. Bakken, C. Adamo, J. Jaramillo, R. Gomperts, R. E. Stratmann, O. Yazyev, A. J. Austin, R. Cammi, C. Pomelli, J. W. Ochterski, R. L. Martin, K. Morokuma, V. G. Zakrzewski, G. A. Voth, P. Salvador, J. J. Dannenberg, S. Dapprich, A. D. Daniels, O. Farkas, J. B. Foresman, J. V. Ortiz, J. Cioslowski and D. J. Fox, Gaussian 09, Revision A.02, Gaussian, Inc., Wallingford CT, 2009.

2 D. Van Der Spoel, E. Lindahl, B. Hess, G. Groenhof, A. E. Mark, H. J. Berendsen, J. Comput. Chem. 2005, **26**, 1701-1718.

3 C. I. Bayly, P. Cieplak, W. Cornell, P. A. Kollman, J. Phys. Chem. 1993, **97**, 10269.

4 J. Wang, R. M. Wolf, J. W. Caldwell, P. A. Kollman, D. A. Case, J. Comput. Chem. 2004, **25**, 1157.

5 T. Lu, F. Chen, J. Comput. Chem. 2012, **33**, 580.

6 C. Fonseca Guerra, J. G. Snijders, G. Te Velde, E. J. Baerends, Theor. Chem. Acc 1998, **99**, 391.

7 G. Kresse, J. Furthmüller, Comput. Mater. Sci. 1996, **6**, 15.

8 G. Kresse, J. Furthmüller, Phys. Rev. B 1996, **54**, 11169.

9 J. P. Perdew, K. Burke, M. Ernzerhof, Phys. Rev. Lett. 1996, 77, 3865.

10 T. Lu, F. Chen, J. Comput. Chem. 2012, 33, 580.